

Data Acquisition System for Indoor Air Quality Monitoring using Arduino UNO R3 Board

Erick Andrés Obregón Fonseca

March 11, 2024

Abstract

In recent years, scientists, politicians, and environmental institutions have focused on Indoor Air Quality. Later research has demonstrated that poor air quality can lead to different respiratory problems and cardiovascular diseases. This project aims to develop a prototype for an Indoor Air Quality Monitoring System using an Arduino UNO board. For such a task, variables like temperature, humidity, and gas concentrations are measured to detect any condition that can cause long-term health issues. First, some basic concepts are introduced. Then, the following methodology is described, where the development of the system is shown. This includes the choice of sensor, design of amplification, and filtering stages for analog sensor, and the proposed algorithm for data sampling. Finally, the results and conclusions are discussed regarding the design of the conditioning and filtering stage of the analog sensor.

Keywords— Arduino UNO, DAQ system, I2C, IQA, sensors

Contents

1	Introduction	2
2	Methodology	2
2.1	Project Requirements	2
2.2	Developed Methodology	3
3	Results and Discussion	11
4	Conclusion	11

1 Introduction

In recent decades, the attention on Indoor Air Quality (IAQ) has become a focal point for scientific researchers, political institutions, and environmental regulators worldwide. This heightened interest aims to improve the living conditions, health, and well-being of individuals residing in buildings. Numerous research efforts have indicated both qualitative and quantitative changes in IAQ over time, emphasizing an increase in pollutants and their concentrations. An estimation showed that individuals spend approximately 90% of their time in various indoor environments, including homes, gyms, schools, workplaces, and vehicles. Consequently, IAQ significantly influences health and overall quality of life. For many people, the health hazards associated with indoor air pollution may surpass those linked to outdoor pollution. Specifically, poor IAQ can pose a significant risk to vulnerable demographics such as children, young adults, the elderly, and those with chronic respiratory or cardiovascular conditions [1]. This is why monitoring the IAQ is important.

Data Acquisition (DAQ) System samples signals containing real-world physical conditions—like voltage or current—and converts them into digital signals that can be handled for another device. Many signals that are sampled from sensors and transducers must be conditioned before they can be transformed into digital signals [2]. A signal conditioning circuit is designed to convert a signal from the sensing element up to a format that can be processed by the load device, usually an Analog-Digital Converter (ADC). For effective operation, a signal conditioner must dutifully serve two entities: the sensor and the load device. The input characteristics of the signal conditioner should match the output characteristics of the sensor, while its output should produce a voltage that can easily be interfaced with an ADC or another load device [3]. Developing a DAQ System that can monitor the IAQ is the main goal of this work.

Arduino UNO Rev 3 is a microcontroller board based on the ATmega328P that has 14 digital input/output pins (of which 6 can be used as Pulse-Width Modulation (PWM) outputs), 6 analog inputs, a 16 MHz ceramic resonator, a Universal Serial Bus (USB) connection, a power jack, an In-Circuit Serial Programming (ICSP) header, and a reset button [4]. The ATmega328P datasheet [5] indicates it contains a successive approximation ADC with a resolution of 10-bit. The ADC is connected to an 8-channel analog multiplexer which allows eight single-ended voltage inputs constructed from the pins of Port A [5].

2 Methodology

In this section, the project requirements and the following methodology are described.

2.1 Project Requirements

The design must include the following features:

1. The system requires an analog sensor with a voltage, current, resistance, capacitance or inductance output, and a sensor that connects to a data bus (Serial Peripheral Interface (SPI) or Inter-Integrated Circuit (I2C)). The aim is for the application to be relevant, that is, to have a practical use. There are no restrictions regarding the different sensors being complementary (for example, measuring temperature). The sensors to be used, even if done theoretically, will be real sensors, and, therefore, must be based on the data sheets of each sensor chosen for the work and simulations. Selection of each of the sensors and justification must be given.
2. Selection of data sample device. The system is intended to sample sensor values on some type of data sample device.
3. Design of signal connectors, including their conditioning when necessary.
4. Demonstrate, in the case of the analog sensor, that the conditioning is working properly (for example, the output voltage is correct). Choose a filter type, investigate its implementation, and justify the choice according to the application to be made. Take into consideration that amplifiers should not be considered ideal, and parameters must be configured. A virtual amplifier can be used, but its values must be configured concerning a real amplifier.
5. Design of an algorithm for data collection. Take into consideration energy management modes when using the system.
6. Design of the complete system at the connection level (that is, to understand it better, the design at a level that would allow proceeding to the design of a Printed Circuit Board (PCB)).

2.2 Developed Methodology

In this section, the selection of the sensors, the data sample device, and the design decisions are described. Also, the developed algorithm for data collection is shown.

2.2.1 Sensors

First of all, the selected variables to measure the IAQ were the temperature, humidity, and gas concentrations. High temperatures can affect the exhaled CO₂ concentration, a harmful air pollutant, as well as an increase in the pulse rate [6]. Some studies have shown a correlation between coarse particulate matter and relative humidity [7, 8, 9]. Humidity can affect particle concentration by influencing the formation, growth, and behavior of particles in the atmosphere, as well as the dispersion and transportation of such particles [8]. This particle concentration can cause respiratory symptoms—like coughing, wheezing, and shortness of breath—and cardiovascular problems—like atherosclerosis and heart attacks—with long-term effects [10, 11, 12].

To measure those variables, the following sensors were selected:

- **MQ-2 Gas Sensor:** It is an analog sensor designed to detect smoke and flammable gases. It is primarily utilized in home gas leak alarms and detectors due to its heightened responsiveness to propane and smoke. Some good characteristics of the MQ-2 sensor are [13, 14]:
 1. **Versatility:** It is capable of detecting a variety of flammable gases and smoke making it useful for a range of applications in family and industry.
 2. **Sensitivity:** It has high sensitivity to gases such Liquefied Petroleum Gas (LPG), i-butane, propane, methane, alcohol, Hydrogen, making it ideal for air quality monitoring. As shown in the datasheet [13]:
 - 200ppm-5000ppm LPG and propane.
 - 300ppm-5000ppm butane.
 - 5000ppm-20000ppm methane.
 - 300ppm-5000ppm H₂
 - 100ppm-2000ppm Alcohol
 3. **Ease of use:** It is easy to use and interface with microcontrollers like Arduino. It provides an analog output that can be read directly by an analog pin on the Arduino.
 4. **Availability:** It is widely available and relatively inexpensive, making it an attractive option for many Do It Yourself (DIY) projects and commercial applications.
- **BMP180 Barometric Pressure Sensor:** It is a high-precision sensor designed for consumer applications used to measure barometric or atmospheric pressure [15]. The BMP180 sensor senses that pressure and provides that information in digital output [16]. Since the temperature also affects the pressure, the BMP180 sensor has a good temperature sensor to compensate for pressure readings [15]. Some advantages of the BMP180 sensor are [15, 16]:
 1. **Versatility:** It can measure both temperature and altitude, making it useful for various applications.
 2. **High Relative Accuracy:** It has a high relative accuracy of $\pm 0.12\text{hPa}$, making it reliable for precise measurements.
 3. **Low Power Consumption:** It consumes very little power ($3\mu\text{A}$), making it ideal for battery-operated systems like smartwatches and mobile phones.
 4. **Fast Communication:** It is capable of communicating with a high-speed Two Wire Interface (TWI) with a 3.4Mhz interface, making it suitable for applications where high-speed communication is needed.
 5. **Wide Operating Temperature Range:** It can operate in a wide temperature range from -40°C to $+80^{\circ}\text{C}$.

2.2.2 Data Sample Device

Gas sensors can be affected by Low-Frequency Noise (LFN) coming from different sources, including flicker noise (pink noise or $1/f$ noise) and thermal noise (Johnson-Nyquist noise) [17, 18, 19].

Flicker noise can be observed in various electronic devices and systems—including chemoresistive-based sensors—and it decreases as the frequency increases. In the context of gas sensing, resistance fluctuations in the sensing materials can be measured as low-frequency noise, typically up to a few kHz. The intensity and slope of the power spectral density of the flicker noise can enhance gas sensing capabilities. Different measurement setups and noise-processing methods are used for gas detection in resistive gas sensors, depending on the Direct Current (DC) resistance of the sensing materials [17, 20]. In well-designed systems, Flicker noise is generally the primary source at lower frequencies, whereas white noise tends to prevail at higher frequencies [21]. In Fig 1, how a Power Spectral Density (PSD) of a system output looks like is shown [21].

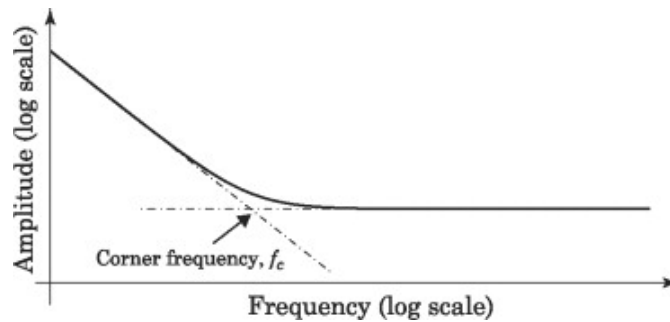


Figure 1: A typical PSD for the noise at the output of a system in the presence of both Flicker and white noise sources.

The corner frequency (f_c) is the frequency at which the Flicker noise and the white noise of a system are equal in magnitude and is a key parameter in characterizing the noise performance of electronic devices [19]. For the MQ-2 gas sensor specifically, it would need to conduct noise measurements and spectral analysis. This involves measuring the output voltage of the sensor over a range of frequencies and plotting the noise spectral density. Since this is out of the project scope, based on [19] findings, a value of 10kHz is assumed for this project. Having said that a high-pass filter will be used to filter the noise of the signal.

Butterworth filter is characterized by a smooth roll-off and a flat response in the passband, which means that it attenuates frequencies outside the passband without introducing ripples or distortions [22]. This filter might not be the best choice for Flicker noise because of its maximally flat frequency response and Flicker noise is more prominent at lower frequencies, and a filter with a sharper cutoff might be more beneficial. Chebyshev filter is a type of Infinite Impulse Response (IIR) filter that provides a steeper roll-off in the stopband compared to Butterworth filter [23]. However, the passband ripples can cause additional noise. Bessel filter is a type of low-pass filter that exhibits a maximally flat frequency response in the passband, meaning that the magnitude response is nearly constant up to the cutoff frequency. They also have a linear phase response, meaning that all frequency components of the input signal are delayed by the same amount, preserving the waveform shape [24]. In Fig 2, the comparison for the 3 filters is shown [25].

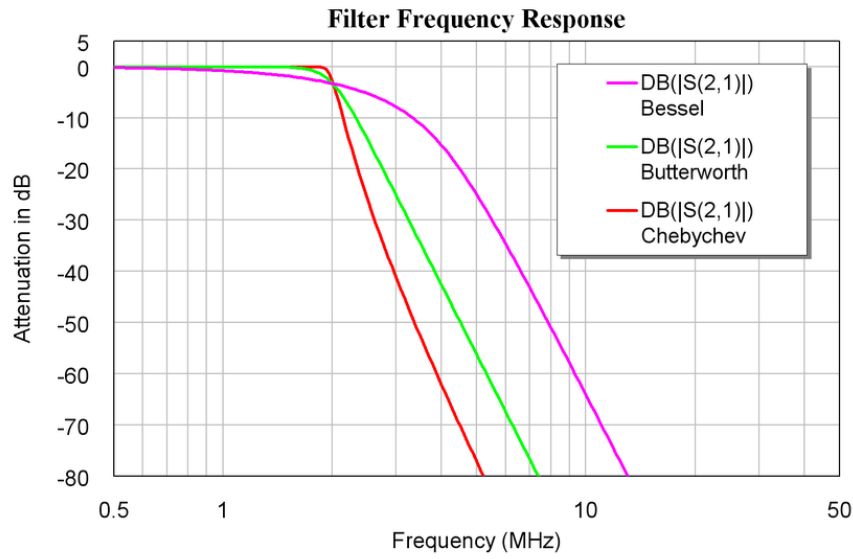


Figure 2: Comparison of Butterworth, Chebyshev, and Bessel filters.

The filter to implement will be a second-order Bessel high-pass filter with a cut-off frequency of 10kHz. The second-order filter was chosen to reduce the complexity of the designed system.

The Filter Design Tool of Texas Instruments [26], can help to save time computing the resistors and capacitors values of the filter topology. Now that the requirements and characteristics of the required filter have been defined, the tool can be used. First, the desired filter needs to be selected:

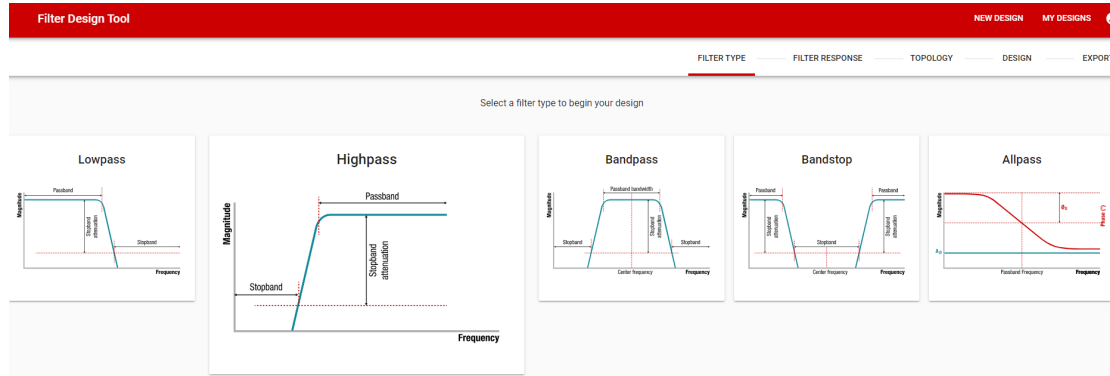


Figure 3: Filter Design Tool–Filter type choice.

Then, the parameters for the filter response can be set. The gain is set to 1 since this stage just takes care of filtering while the amplification stage is discussed in the next section (Sec 2.2.3). The frequency is 10kHz, as discussed previously.

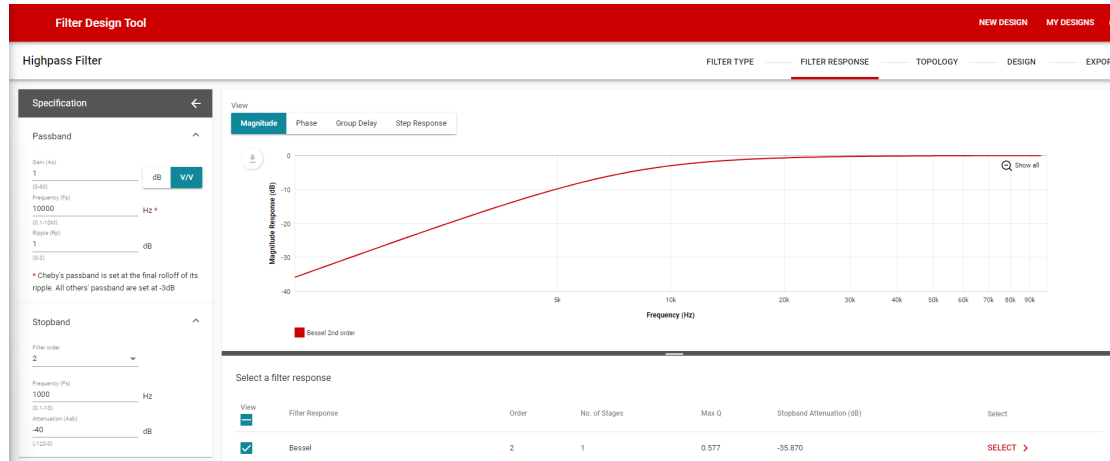
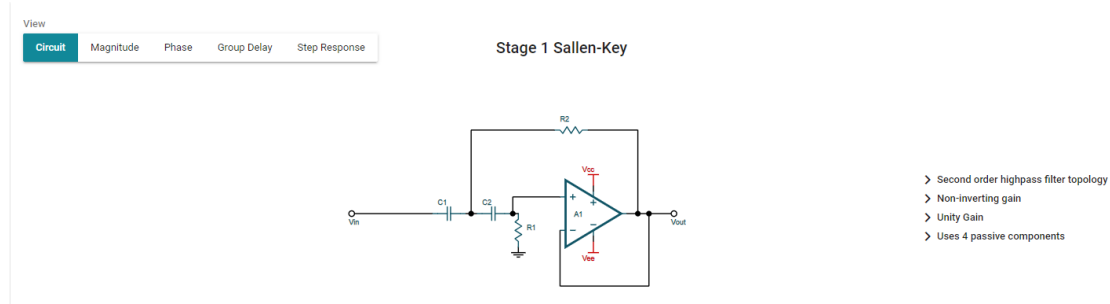
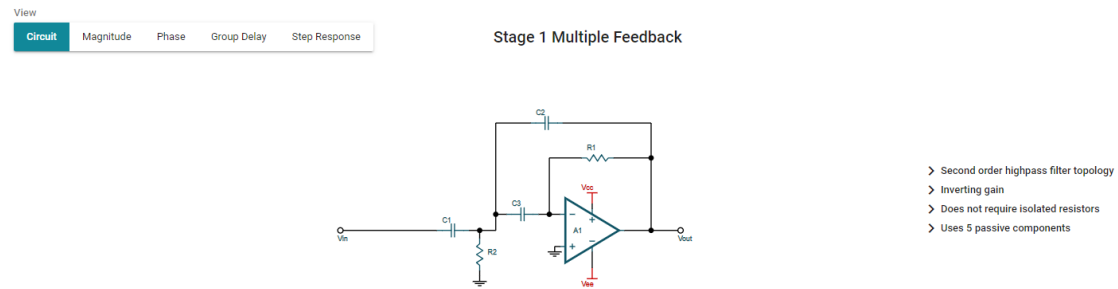


Figure 4: Filter Design Tool–Filter response settings.

The next step is topology selection. The two options are the Sallen-Key and the Multiple Feedback topology. Due to its unity gain and non-inverting gain features, the Sallen-Key topology is used, since the amplified signal won't be inverted.



(a) Filter Design Tool–Topology - Sallen-Key.



(b) Filter Design Tool–Topology - Multiple Feedback.

The operational amplifier selected for this task is the OPA2186. It is due to [27]:

- **Low Offset Voltage ($1\mu\text{V}$):** This minimizes the difference in voltage between the two input terminals when the output is at zero, improving the precision.
- **Zero-Drift Performance:** It maintains stable performance across varying temperatures, ensuring that the offset voltage remains consistent and improving precision in applications.
- **Low Input Bias Current (1pA max):** This is crucial for applications involving high-impedance sources and minimizes the impact on sensitive circuits, ensuring accurate signal processing.
- **Unity-Gain Stable:** It remains stable even when configured with a gain of 1 (no external feedback).
- **Low Quiescent Current ($140\mu\text{A per channel}$):** This is essential for battery-powered devices, as it conserves energy and extends battery life—which is a requirement for the project.

This configuration generates the circuit of Fig 6 with the magnitude response (Fig 7a), the phase response (Fig 7b), the group delay (Fig 7c), and the step response (Fig 7d).

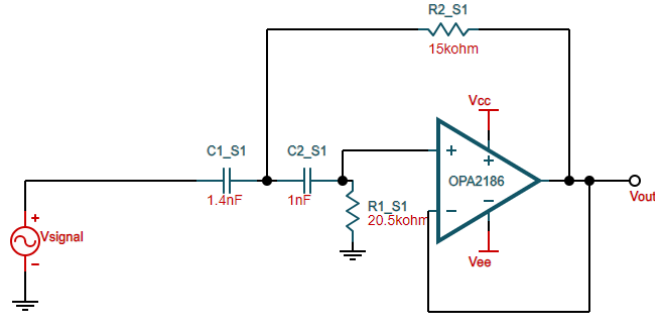
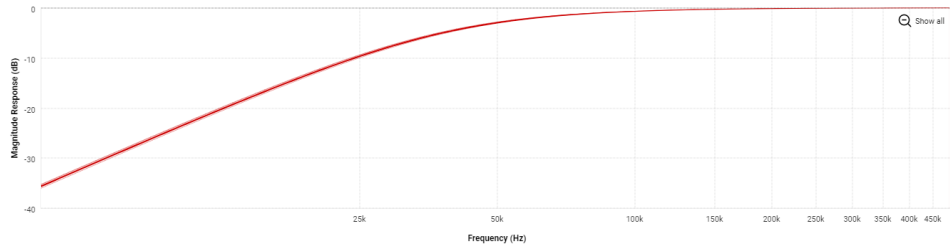
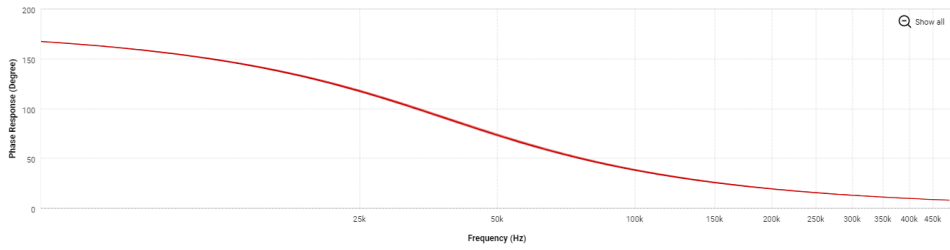


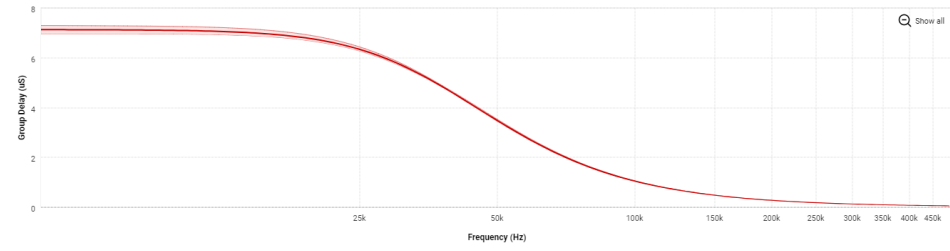
Figure 6: Filter Design Tool–Filter response settings.



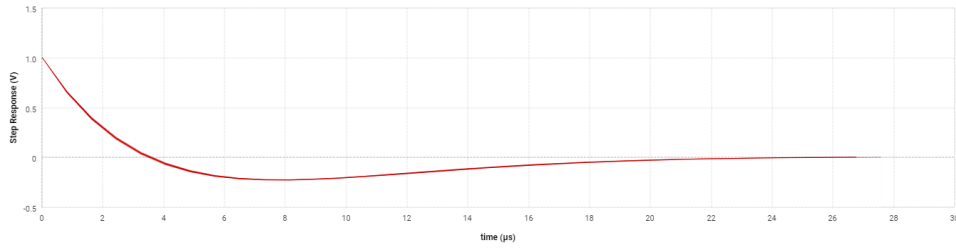
(a) Filter Design Tool–Design–Magnitude response.



(b) Filter Design Tool–Design–Phase response.



(c) Filter Design Tool–Topology–Group delay.



(d) Filter Design Tool–Topology–Step response.

2.2.3 Signal Conditioning

The diagram of the MQ-2 sensor can be obtained from its datasheet (Fig 8) [13].

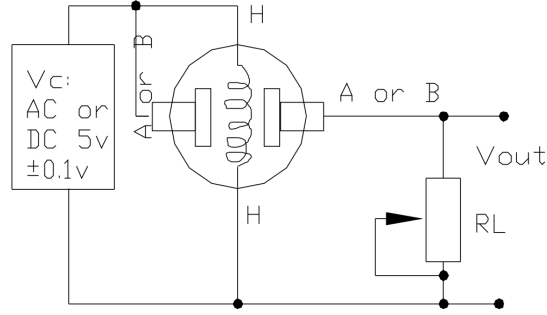


Figure 8: MQ-2 sensor diagram.

The MQ-2 datasheet also mentions that the sensor requires calibration. For such a task, the manufacturer provided the typical sensitivity characteristics of the MQ-2 for several gases—shown in Fig 9. The values are set to:

- Temp: 20°C.
- Humidity: 65%.
- O₂ concentration: 21%
- R_L: 5kΩ
- R_O: sensor resistance at 1000ppm of H₂ in the clean air.
- R_S: sensor resistance at various concentrations gases.
- V_C: circuit voltage (5V).

The output voltage V_{out} is obtained from the voltage division of the load resistor R_L (can adjust) and the sensor resistance R_S . Based on that:

$$V_{out} = \frac{R_L}{R_L + R_S} V_C \quad (1)$$

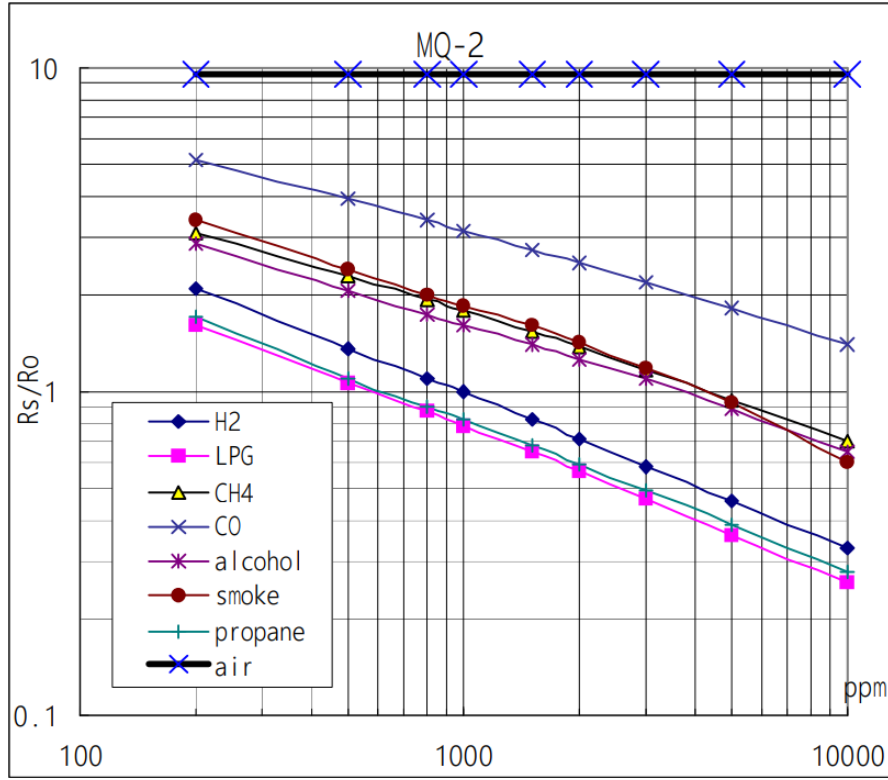


Figure 9: Typical sensitivity characteristics of the MQ-2 sensor for several gases.

After calibrating the MQ-2 sensor using an Arduino UNO Rev 3 and guide provided by [28], a voltage range value of 0 (for 0ppm) to 1V (10000ppm) is obtained. Load resistor R_L was calibrated at $5k\Omega$. Solving R_S from Eq 1:

$$R_S = R_L \cdot \frac{V_{out} - V_S}{V_{out}} \quad (2)$$

Substituting $V_{out} = 0V$ and $R_L = 5k\Omega$ in Eq 2:

$$R_S = \infty\Omega \quad (3)$$

Substituting $V_{out} = 1V$ and $R_L = 5k\Omega$ in Eq 2:

$$R_S = 20k\Omega \quad (4)$$

With this, the output of the system can be modeled as a resistor or a voltage. The most common use of the sensor is a voltage output, so the sensor is modeled in that way.

For the signal amplification, a non-inverting amplifier is used. The topology selected is shown in Fig 10 [29]. For such a task, the operational amplifier LM358 is chosen due to [30]:

- It is a low-power dual operational amplifier with a wide range of power supply voltages (3 to 36V) and good stability—which accomplishes the lower-power consumption requirement for this system.
- Due to its low power consumption, it can operate with a battery or the Arduino UNO supply.
- It features high-gain frequency, which is internally compensated.
- It simplifies the design due to its unity-gain stability, lower-offset voltage (maximum of 3mV), and lower quiescent current of $300\mu A$.

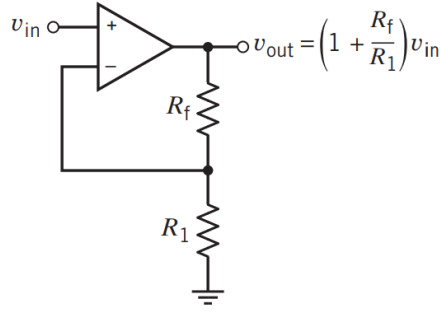


Figure 10: Non-inverting amplifier.

Given the Eq 5 for the non-inverting operational amplifier gain:

$$A = \frac{V_{out}}{V_{in}} = 1 + \frac{R_f}{R_i} \quad (5)$$

The gain of the conditioning circuit must be $A = 5V/V$, such as:

$$R_f = 4R_i \quad (6)$$

To ensure low current and real values of the resistance, $R_f = 39k\Omega$ and $R_i = 10k\Omega$, given a gain $A = 4.9V/V$.

2.2.4 Integration of the System

The system consist of a MQ-2 gas analog sensor connected to a filtering and an amplification stage. After signal conditioning, the output signal is connecte to the Arduino analog pin A3. For the I2C-based BMP180 humidity sensor, the SCL sensor pin is connected to the A5 pin of the Arduino, and the SDA sensor pin is connected to the A4 Arduino pin. To save some power, the VCC pin of each sensor will be connected a digital Arduino pin, which allow the system to power-off the sensor when it is no required. In Fig 11, the whole system integration can be seen at high-level.

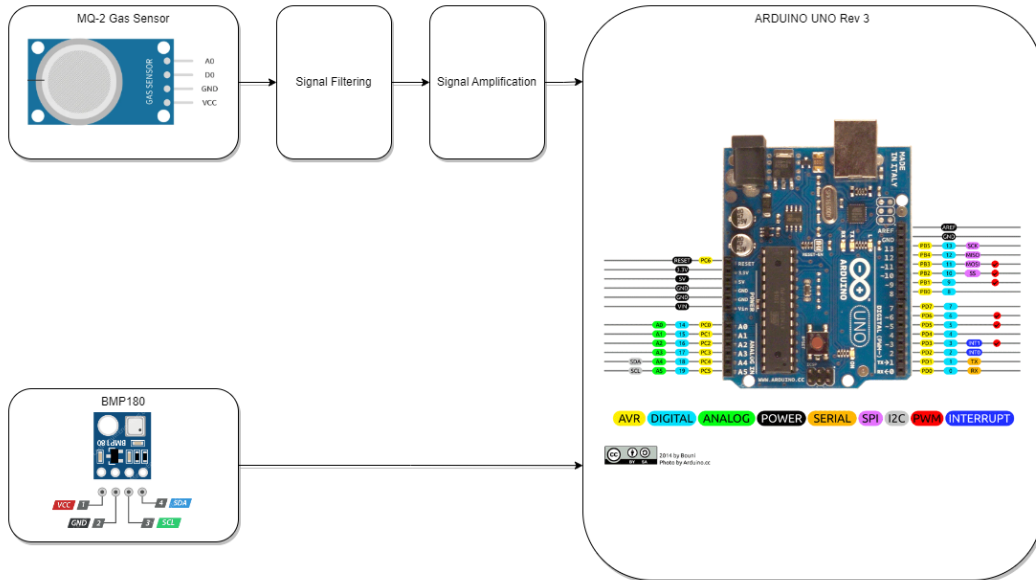


Figure 11: Diagram showing the whole system connected.

2.2.5 Sampling Algorithm

3 Results and Discussion

4 Conclusion

References

- [1] A. Cincinelli and T. Martillini, "Indoor Air Quality and Health," *International Journal of Environmental Research and Public Health*, vol. 1286, no. 14, 2017.
- [2] M. Di Paolo Emilio, *Data Acquisition Systems From Fundamentals to Applied Design*. Springer New York, NY, 1st ed., March 2013.
- [3] J. Fraden, *Handbook of Modern Sensors: Physics, Designs, and Applications*. Springer Cham, 2016.
- [4] Arduino CC, "Arduino UNO R3." <https://docs.arduino.cc/hardware/uno-rev3>.
- [5] Atmel, "ATmega328P - 8-bit AVR Microcontroller with 32K Bytes In-System Programmable Flash - DATASHEET." https://ww1.microchip.com/downloads/en/DeviceDoc/Atmel-7810-Automotive-Microcontrollers-ATmega328P_Datasheet.pdf.
- [6] R. A. Angelova, D. Markov, R. Velichkova, P. Stankov, and I. Simova, "Exhaled carbon dioxide as a physiological source of deterioration of indoor air quality in non-industrial environments: Influence of air temperature," *Energies*, vol. 14, no. 23, 2021.
- [7] L. Yang, S. Hong, C. He, J. Huang, Z. Ye, B. Cai, S. Yu, Y. Wang, and Z. Wang, "Spatio-Temporal Heterogeneity of the Relationships Between PM_{2.5} and Its Determinants: A Case Study of Chinese Cities in Winter of 2020," *Sec. Environmental health and Exposome*, vol. 10, 2022.
- [8] T. Tanatachalert and A. Jumlongkul, "Correlation Between Relative Humidity and Particulate Matter During the Ongoing of Pandemic: A Systematic Review," *Aerosol Sci Eng*, no. 7, 2023.
- [9] Y. F. Xing, Y. H. Xu, M.-H. Shi, and Y. X. Lian, "The impact of PM_{2.5} on the human respiratory system," *National Library of Medicine*, vol. 8, no. 1, 2016.
- [10] S. Ahamed Ibrahim, S. Sri Shalini, A. Ramachandran, and K. Palanivelu, "Spatio-temporal variation and sensitivity analysis of aerosol particulate matter during the COVID-19 phase-wise lockdowns in Indian cities," *Journal of Atmospheric Chemistry*, vol. 79, 2022.
- [11] J. Ding, Q. Dai, Y. Li, S. Han, Y. Zhang, and Y. Feng, "Impact of meteorological condition changes on air quality and particulate chemical composition during the COVID-19 lockdown," *Journal of Environmental Sciences*, vol. 109, pp. 45–56, 2021.
- [12] F. Tan, Y. Guo, W. Zhang, X. Xu, M. Zhang, F. Meng, S. Liu, S. Li, and L. Morawska, "Large-Scale Spraying of Roads with Water Contributes to, Rather Than Prevents, Air Pollution," *Toxics*, vol. 9, no. 6, 2021.
- [13] Hanwei Electronics Co. LTD, "Technical Data MQ-2 Gas Sensor." <https://www.mouser.com/datasheet/2/321/605-00008-MQ-2-Datasheet-370464.pdf>.
- [14] Components101, "MQ2 Gas Sensor." <https://components101.com/sensors/mq2-gas-sensor>, 2018.
- [15] Components101, "BMP180 - Atmospheric Pressure Sensor." <https://components101.com/sensors/bmp180-atmospheric-pressure-sensor>, 2018.
- [16] Bosch Sensortec, "BMP180 Digital pressure sensor Data sheet." <https://www.digikey.com/htmldatasheets/production/856385/0/0/1/bmp180-datasheet.html>, 2012.
- [17] H.-J. Kwon, H. Kang, J. Jang, S. Kim, and C. P. Grigoropoulos, "Analysis of flicker noise in two-dimensional multilayer MoS₂ transistors," *Applied Physics Letters*, vol. 104, p. 083110, 02 2014.
- [18] W. Shin, S. Hong, Y. Jeong, G. Jung, J. Park, D. Kim, K. Choi, H. Shin, R.-H. Koo, J.-J. Kim, and J.-H. Lee, "Low-frequency noise in gas sensors: A review," *Sensors and Actuators B: Chemical*, vol. 383, p. 133551, 2023.
- [19] J. Smulko, G. Scandurra, K. Drozdowska, A. Kwiatkowski, C. Ciofi, and H. Wen, "Flicker Noise in Resistive Gas Sensors—Measurement Setups and Applications for Enhanced Gas Sensing," *Sensors*, vol. 24, no. 2, 2024.
- [20] R. Kiely, "Understanding and Reducing 1/f Noise in Precision Measurement Applications," *Journal of Precision Measurement*, vol. 51, no. 05, 2017.
- [21] B. Bahreyni, "Chapter 7 - noise," in *Fabrication and Design of Resonant Microdevices* (B. Bahreyni, ed.), Micro and Nano Technologies, pp. 129–141, Norwich, NY: William Andrew Publishing, 2009.
- [22] S. Ruofei, "A Design Method of Active High-Pass Butter-worth Filter," in *2021 IEEE International Workshop on Electromagnetics: Applications and Student Innovation Competition (iWEM)*, vol. volume1, pp. 1–3, 2021.

- [23] P. Podder, M. Mehedi Hasan, M. Rafiqul Islam, and M. Sayeed, "Design and Implementation of Butterworth, Chebyshev-I and Elliptic Filter for Speech Signal Analysis," *International Journal of Computer Applications*, vol. 98, pp. 12–18, July 2014.
- [24] A. Soni and M. Gupta, "Analysis and Design of Optimized Fractional Order Low-Pass Bessel Filter," *Journal of Circuits, Systems and Computers*, vol. 30, no. 02, 2021.
- [25] C. Kikkert, "The effect of filter type on BER of WCDMA-UMTS mobile radio systems," pp. 966 – 969, 10 2008.
- [26] Texas Instruments, "Filter Design Tool." <https://webench.ti.com/filter-design-tool/filter-type>.
- [27] Texas Instruments, "OPAx186 Precision, Rail-to-Rail Input/Output, 24-V, Zero-Drift Operational Amplifiers." <https://www.ti.com/lit/ds/symlink/opa2186.pdf?ts=1710119647212>, 2017.
- [28] S. Hu, "Grove - Gas Sensor(MQ2)." https://wiki.seeedstudio.com/Grove-Gas_Sensor-MQ2/, 2023.
- [29] J. A. Svoboda and R. C. Dorf, *Introduction to Electric Circuits*. John Wiley & Sons, 2010, 2013.
- [30] Texas Instruments, "LM358 Datasheet." <https://pdf1.alldatasheet.com/datasheet-pdf/view/1648891/TI/LM358.html>.